Computers and Concrete, *Vol. 21, No. 6 (2018) 717-726*
DOI: https://doi.org/10.12989/cac.2018.21.6.717

Seismic response of concrete beam with smart layer using DQ and Newmark methods

Reza Taherifar*[1], Shabnam Nasr Esfahani[2], Mohammad Hossein Nasr Esfahani[3], Farhad Chinaei[4] and Maryam Mahmoudi[5]

[1]*Department of Civil Engineering, Meymeh Branch, Islamic Azad University, Meymeh Iran*
[2]*Department of Electrical Engineering, Meymeh Branch, Islamic Azad University, Meymeh Iran*
[3]*Department of Mathematics, Faculty of Basic Science, Meymeh Branch, Islamic Azad University, Meymeh Iran*
[4]*Department of Civil and Mineral Engineering, Meymeh Branch, Islamic Azad University, Meymeh Iran*
[5]*Department of Computer Engineering, Meymeh Branch, Islamic Azad University, Meymeh Iran*

(Received September 17, 2017, Revised March 5, 2018, Accepted March 23, 2018)

Abstract. Concrete pipelines are the most efficient and safe means for gas and oil transportation over a long distance. The use of nano materials and nono-engineering can be considered for enhancing concrete pipelines properties. the tests show that SiO_2 nanoparticles can improve the mechanical behavior of concrete. Moreover, severe hazard for pipelines is seismic ground motion. Over the years, scientists have attempted to understand pipe behavior against earthquake most frequently via numerical modeling and simulation. Therefore, in this paper, the dynamic response of underwater nanocomposite submerged pipeline conveying fluid is studied. The structure is subjected to the dynamic loads caused by earthquake and the governing equations of the system are derived using mathematical model via Classic shell theory and Hamilton's principle. Navier-Stokes equation is employed to calculate the force due to the fluid in the pipe. As well, the effect of external fluid is modeled with an external force. Mori-Tanaka approach is used to estimate the equivalent material properties of the nanocomposite. 1978 Tabas earthquake in Iran is considered for modelling seismic load. The dynamic displacement of the structure is extracted using differential quadrature method (DQM) and Newmark method. The effects of different parameters such as SiO_2 nanoparticles volume percent, boundary conditions, thickness to radius ratios, length to radius ratios, internal and external fluid pressure and earthquake intensity are discussed on the seismic response of the structure. From results obtained in this paper, it can be found that the dynamic response of the pipe is increased in the presence of internal and external fluid. Furthermore, the use of SiO_2 nanoparticles in concrete pipeline reduces the displacement of the structure during an earthquake.

Keywords: dynamic response; concrete pipeline; Tabas earthquake; internal and external fluid; Differential Quadrature method

1. Introduction

Fluid-conveying submerged cylindrical pipes have been widely used in many civil and mechanical engineering applications for example in the submarine industry, oil and gas industry, petrochemicals systems, and so on. Such cylindrical structures have been analyzed for many of the failures and/or operating problems due to flow-induced vibrations and instabilities from previous decades (Housner 1952, Benjamin 1961, Païdoussis and Issid 1974). In the last years, some studies have been done on the dynamic characteristics of sensor, pipelines, ultrasonic devices and computer programs (Amabili *et al*. 1999a, 1999b, 2000, 2003, 2008, Païdoussis *et al*. 2004, 2005, 2007a, 2007b, Lopes *et al*. 2002, Semler *et al*. 2002, Yang and Yu 2017, Li *et al*. 2017, Padhy and Panda 2017, Zhao *et al.* 2017, Rishikeshan and Ramesh 2017, Wen *et al*. 2017, Torres-Jimenez and Rodriguez-Cristerna 2017, Liu *et al*. 2018). Also, several studies have been performed on the dynamical response of the submerged pipes and/or fluid conveying pipes against underwater shock, effect of the moving mass, fluid induced vibrations and ground motion acceleration that is noted as follows.

Gong *et al*. (2000) applied a computational method for safety evaluation of submerged pipelines, subjected to underwater shock. In this research, the fluid structure interaction between the pipeline and sea water were considered based on the coupled boundary-element and finite-element programs, by means of the Doubly Asymptotic Approximation (DAA). Lee and Oh (2003) developed a spectral element model for the pipe conveying fluid to study the flow induced vibrations of the system by the exact constitutive dynamic stiffness matrix. Lam *et al.* (2003) examined the dynamic response of a simply supported laminated underwater pipeline exposed to underwater explosion shock. They concluded that the strength of the radial direction for the pipe is weaker than the strengths in the longitudinal and the circumferential directions. Consequently, the dynamic response of the radial direction is larger than those of other directions. Yoon and Son (2007) studied the dynamic behavior of simply supported fluid-conveying pipe in due to the effect of the open crack and the moving mass. Lin and Qiao (2008)

*Corresponding author, Professor
E-mail: m.rabanibidgoli@gmail.com

ISSN: 1598-8198 (Print), 1598-818X (Online)

explored vibration and instability of an axially moving beam immersed in fluid with simply supported conditions along with torsional springs. The transient reaction of submerged thin shell subjected to mechanical excitations was studied by Leblond and Sigrist (2010). Huang *et al.* (2010) used Galerkin's method to obtain eigen frequencies of tubes conveying fluid having different boundary conditions. Further, they calculated the variation of system eigen frequencies by the effect of the Coriolis forces and expressed a correlation between a pipe conveying fluid and Euler-Bernoulli beam. Zhai *et al.* (2011) used the Timoshenko beam model for obtaining the dynamic response of a fluid-conveying pipe under random excitation. They solved the governing equations by the pseudo excitation method together with complex mode superposition method. Also, they assumed that the parameters of load are random. Liu *et al.* (2012) analyzed fluid-solid interaction problem for an elastic cylinder by numerical simulations and acquired the vibration of cylinder for both laminar and turbulent flows. Dynamic behaviour investigation of pipelines under earthquake acceleration is a research field with few works. Seismic response of natural gas and water pipelines in the Ji-Ji earthquake was considered by Chen *et al.* (2002). They conducted a Statistical analysis for understanding the relationship between seismic factors (the spectrum intensity, peak ground acceleration and peak ground velocity) and repair rates. Also, Abdoun *et al.* (2009) studied influencing factors on the behavior of buried pipelines subjected to earthquake faulting. In none of mentioned investigations, the structure is not composite. Effect of using fiber-reinforced polymer composites for underwater steel pipeline repairs was studied by Shamsuddoha *et al.* (2013). They offered a widespread review about of using fiber-reinforced polymer composites for in-air, underground and underwater pipeline repairs. Ray and Reddy (2013) made a study on the active damping of piezoelectric composite cylindrical shells conveying fluid. Alijani and Amabili (2014) used energy method with the Amabili-Reddy nonlinear higher-order shear deformation theory for determining the nonlinear vibrations and multiple resonances of fluid filled arbitrary laminated cylindrical shells. They demonstrated that water-filled composite shells may exhibit complex nonlinear dynamic behaviour. Thinh and Nguyen (2016) investigated the free vibration of composite circular shells containing fluid. They used the Dynamic Stiffness Method (DSM) based on the Reissner-Mindlin theory and non-viscous incompressible fluid equations for modelling of structure. Dynamic characteristic of steady fluid conveying in the periodical partially viscoelastic composite pipeline was studied by Zhou *et al.* (2017). It is shown that the reducing of coverage fraction decreases the flutter velocity. Non-linear vibration of laminated composite circular cylindrical shells using Donnell's shell theory and Incremental Harmonic Balance (IHB) method was analyzed by Dey and Ramachandram (2017). Furthermore, the mechanical behavior of concrete structures containing nanoparticles has been investigated experimentally and analytically by a number of researchers. The influences of nanoparticles on dynamic strength of ultra-high performance concrete was tested by Su *et al.* (2016). Jafarian Arani and Kolahchi (2016) studied buckling analysis of concrete columns reinforced with carbon nanotubes by using Euler-Bernoulli and Timoshenko beam models. Buckling of concrete columns retrofitted with Nano-Fiber Reinforced Polymer was investigated by Safari Bilouei *et al.* (2016). Inozemtcev *et al.* (2017) improved the properties of lightweight concrete with hollow microspheres with the nanoscale modifier. Mathematical modeling of concrete pipes reinforced with CNTs conveying fluid for vibration and stability analysis was done by Zamani Nouri (2017). Vibration of Silica nanoparticles-reinforced concrete beams considering agglomeration effects was considered by Shokravi (2017). Also, Rabani Bidgoli and Saeidifar (2017) studied time-dependent buckling of SiO_2 nanoparticles reinforced concrete columns exposed to fire. Recently, Seismic response of SiO_2 nanoparticles-reinforced concrete surface pipes was investigated by Motezaker and Kolahchi (2017). In this research, the concrete pipes were unsubmerged.

Hitherto, the dynamic behavior of the nanocomposite submerged pipes conveying fluid under earthquake load has not been investigated by any researcher. So in this research, for the first time, the seismic response of the nanocomposite submerged pipe conveying fluid under earthquake load is analytically considered as the importance of the subject. Mori-Tanaka method is used to evaluate the material properties of the nanocomposite. The governing equations of the structure are derived using energy method and according to classical theory. The dynamic displacement of the structure is derived using differential quadrature method (DQM) and Newmark method. In present study, effect of various parameters like volume percent of SiO_2 nanoparticles, boundary conditions, geometrical parameters of pipe, internal and external fluid pressure and earthquake intensity on the dynamic displacement of the structure is presented.

2. Mathematical modeling

As shown in Fig. 1, an underwater nanocomposite cylindrical pipe conveying fluid with length a, radius R and thickness h is considered. The geometrical properties of the

Fig. 1 Schematic of underwater concrete pipe conveying fluid

nanocomposite pipe are set as: length to radius ratio: a/R=10, thickness to radius ratio: h/R=0.03. The boundary conditions are simply supported and SiO_2 nanoparticles volume percent is 0.05 unless otherwise specified.

2.1 Strain-displacement relationships

In order to calculate the middle-surface strain and curvatures, using Kirchhoff-Law assumptions, the displacement components of cylindrical shell in the axial x, circumferential θ, and radial z directions can be written as (Brush and Almroth 1975)

$$u_1(x,\theta,z,t)=u(x,\theta,t)-z\frac{\partial w(x,\theta,t)}{\partial x}, \tag{1}$$

$$u_2(x,\theta,z,t)=v(x,\theta,t)-\frac{z}{R}\frac{\partial w(x,\theta,t)}{\partial \theta}, \tag{2}$$

$$u_3(x,\theta,z,t)=w(x,\theta,t), \tag{3}$$

where (u_1,u_2,u_3) denotes the displacement components at an arbitrary point (x,θ,z) in the shell, and (u,v,w) are the displacement components of the middle surface of the shell in the axial, circumferential and radial directions, respectively. Also, z is the distance from an arbitrary point to the middle surface. Using Donnell's linear theory and applying Eqs. (1)-(3), strain-displacement relationships may be written as

$$\varepsilon_{xx}=\frac{\partial u}{\partial x}-z\frac{\partial^2 w}{\partial x^2}, \tag{4}$$

$$\varepsilon_{\theta\theta}=\frac{\partial v}{R\partial\theta}+\frac{w}{R}-\frac{z}{R^2}\frac{\partial^2 w}{\partial\theta^2}, \tag{5}$$

$$\varepsilon_{xy}=\frac{1}{2}\left(\frac{\partial u}{R\partial\theta}+\frac{\partial v}{\partial x}\right)-z\frac{\partial^2 w}{R\partial x\partial\theta}, \tag{6}$$

where (ε_{xx}, $\varepsilon_{\theta\theta}$) are the normal strain components and ($\varepsilon_{x\theta}$) is the shear strain component.

The constitutive equation for stresses σ and strains ε matrix may be written as follows

$$\begin{bmatrix}\sigma_{xx}\\ \sigma_{\theta\theta}\\ \tau_{x\theta}\end{bmatrix}=\begin{bmatrix}C_{11} & C_{12} & 0\\ C_{21} & C_{22} & 0\\ 0 & 0 & C_{66}\end{bmatrix}\begin{bmatrix}\varepsilon_{xx}\\ \varepsilon_{\theta\theta}\\ \gamma_{x\theta}\end{bmatrix}, \tag{7}$$

2.2 Mori-Tanaka rule

In this section, the effective modulus of the concrete pipe strengthened by SiO_2 nano-particles is illustrated. The SiO_2nano-particles are assumed with uniform distribution in the concrete. The matrix is assumed to be elastic and isotropic, with the Young's modulus and the Poisson's ratio E_m, υ_m respectively. The resulting relations for the composite are (Mori and Tanaka 1973)

$$\begin{Bmatrix}\sigma_{xx}\\ \sigma_{yy}\\ \sigma_{zz}\\ \sigma_{yz}\\ \sigma_{xz}\\ \sigma_{xy}\end{Bmatrix}=\begin{bmatrix}k+m & l & k-m & 0 & 0 & 0\\ C_{11} & C_{12} & C_{13} & & & \\ l & n & l & 0 & 0 & 0\\ C_{21} & C_{22} & C_{23} & & & \\ k-m & l & k+m & 0 & 0 & 0\\ C_{31} & C_{32} & C_{33} & & & \\ 0 & 0 & 0 & p & 0 & 0\\ & & & C_{44} & & \\ 0 & 0 & 0 & 0 & m & 0\\ & & & & C_{55} & \\ 0 & 0 & 0 & 0 & 0 & p\\ & & & & & C_{66}\end{bmatrix}\begin{Bmatrix}\varepsilon_{xx}\\ \varepsilon_{yy}\\ \varepsilon_{zz}\\ \gamma_{yz}\\ \gamma_{xz}\\ \gamma_{xy}\end{Bmatrix}, \tag{8}$$

where σ_{ij}, ε_{ij}, γ_{ij}, k, m, n, l, p are the stress components, the strain components and the stiffness coefficients, respectively. According to the Mori-Tanaka method, the stiffness coefficients are given by Mori and Tanaka (1973)

$$\begin{aligned}
k&=\frac{E_m\{E_m c_m+2k_r(1+\nu_m)[1+c_r(1-2\nu_m)]\}}{2(1+\nu_m)[E_m(1+c_r-2\nu_m)+2c_m k_r(1-\nu_m-2\nu_m^2)]}\\
l&=\frac{E_m\{c_m\nu_m[E_m+2k_r(1+\nu_m)]+2c_r l_r(1-\nu_m^2)]\}}{(1+\nu_m)[E_m(1+c_r-2\nu_m)+2c_m k_r(1-\nu_m-2\nu_m^2)]}\\
n&=\frac{E_m^2 c_m(1+c_r-c_m\nu_m)+2c_m c_r(k_r n_r-l_r^2)(1+\nu_m)^2(1-2\nu_m)}{(1+\nu_m)[E_m(1+c_r-2\nu_m)+2c_m k_r(1-\nu_m-2\nu_m^2)]}\\
&\quad+\frac{E_m[2c_m^2 k_r(1-\nu_m)+c_r n_r(1+c_r-2\nu_m)-4c_m l_r\nu_m]}{E_m(1+c_r-2\nu_m)+2c_m k_r(1-\nu_m-2\nu_m^2)}\\
p&=\frac{E_m[E_m c_m+2p_r(1+\nu_m)(1+c_r)]}{2(1+\nu_m)[E_m(1+c_r)+2c_m p_r(1+\nu_m)]}\\
m&=\frac{E_m[E_m c_m+2m_r(1+\nu_m)(3+c_r-4\nu_m)]}{2(1+\nu_m)\{E_m[c_m+4c_r(1-\nu_m)]+2c_m m_r(3-\nu_m-4\nu_m^2)\}}
\end{aligned} \tag{9}$$

where C_m and C_r are the volume fractions of the concrete and the SiO_2nano-particles, respectively. Also k_r, l_r, n_r, p_r, m_r are the Hills elastic modulus for the SiO_2nano-particles (Mori and Tanaka (1973)).

3. Motion equations

In this part, the governing equation of motion can be obtained using energy method.

3.1 Energy method

The total potential energy, V, of the underwater cylindrical shell conveying fluid is the sum of strain energy U, kinetic energy K, and the work done by the fluid W.

The strain energy can be written as

$$U=\int_V\left(\sigma_{xx}\varepsilon_{xx}+\sigma_{\theta\theta}\varepsilon_{\theta\theta}+\sigma_{x\theta}\gamma_{x\theta}\right)dV, \tag{10}$$

By substituting Eqs. (4)-(6) into (10) yields

$$U=\int_{-\frac{h}{2}}^{\frac{h}{2}}\int_A\left(\sigma_x\left(\frac{\partial u}{\partial x}+0.5\left(\frac{\partial w}{\partial x}\right)^2-z\frac{\partial^2 w}{\partial x^2}\right)\right.$$

$$+\sigma_\theta\left(\frac{\partial v}{R\partial\theta}+\frac{w}{R}+0.5\left(\frac{\partial w}{R\partial\theta}\right)^2-z\frac{\partial^2 w}{R^2\partial\theta^2}\right)$$

$$+\sigma_{x\theta}\left(\frac{\partial u}{R\partial\theta}+\frac{\partial v}{\partial x}+\frac{\partial w}{R\partial\theta}\frac{\partial w}{\partial x}-2z\frac{\partial^2 w}{R\partial\theta\partial x}\right)\Bigg)dz\,dA \quad (11)$$

By introducing force and moment resultants asEqs. (12-13) and substituting in Eq. (11), Eq. (14) yields

$$\begin{Bmatrix}N_x\\N_\theta\\N_{x\theta}\end{Bmatrix}=\int_{-\frac{h}{2}}^{\frac{h}{2}}\begin{Bmatrix}\sigma_x\\\sigma_\theta\\\tau_{x\theta}\end{Bmatrix}dz, \quad (12)$$

$$\begin{Bmatrix}M_x\\M_\theta\\M_{x\theta}\end{Bmatrix}=\int_{-\frac{h}{2}}^{\frac{h}{2}}\begin{Bmatrix}\sigma_x\\\sigma_\theta\\\tau_{x\theta}\end{Bmatrix}zdz, \quad (13)$$

$$U=\int_A\Bigg(N_x\left(\frac{\partial u}{\partial x}+0.5\left(\frac{\partial w}{\partial x}\right)^2\right)-M_x\frac{\partial^2 w}{\partial x^2}$$
$$+N_\theta\left(\frac{\partial v}{R\partial\theta}+\frac{w}{R}+0.5\left(\frac{\partial w}{R\partial\theta}\right)^2\right)-M_\theta\frac{\partial^2 w}{R^2\partial\theta^2} \quad (14)$$
$$+N_{x\theta}\left(\frac{\partial u}{R\partial\theta}+\frac{\partial v}{\partial x}+\frac{\partial w}{R\partial\theta}\frac{\partial w}{\partial x}\right)-2M_{x\theta}\frac{\partial^2 w}{R\partial\theta\partial x}\Bigg)dA$$

The kinetic energy may be expressed as

$$K=\frac{\rho}{2}\int_v\left((\frac{\partial u_1}{\partial t})^2+(\frac{\partial u_2}{\partial t})^2+(\frac{\partial u_3}{\partial t})^2\right)dV, \quad (15)$$

By substituting Eqs. (1)-(3) into (15) and defining the following term

$$\begin{Bmatrix}h\\0\\\frac{h^3}{12}\end{Bmatrix}=\int_{-h/2}^{h/2}\begin{bmatrix}1\\z\\z^2\end{bmatrix}dz, \quad (16)$$

We have

$$K=\int\Bigg(\frac{\rho}{2}\left(\frac{h^3}{12}\left((\frac{\partial^2 u}{\partial t\,\partial x})^2+(\frac{\partial^2 w}{\partial t\partial\theta})^2\right)\right)$$
$$+h\left((\frac{\partial u}{\partial t})^2+(\frac{\partial v}{\partial t})^2+(\frac{\partial w}{\partial t})^2\right)\Bigg)dA. \quad (17)$$

The external work due to internal Newtonian fluid can be obtained using the well-known Navier-Stokes equation as below (Ghorbanpour Arani *et al*. 2013)

$$\rho_f\frac{d\mathbf{V}}{dt}=-\nabla\mathbf{P}+\mu\nabla^2\mathbf{V}+\mathbf{F}_{body}, \quad (18)$$

where V=(v_x, v_θ, v_z) is the flow velocity vector in cylindrical coordinate system with components in longitudinal x, circumferential θ and radial z directions. Also, P, $\theta$and ρ_f are the pressure, the viscosity and the density of the fluid, respectively and F_{body} denotes the body forces. In Navier-Stokes equation, the total derivative operator with respect to t is

$$\frac{d}{dt}=\frac{\partial}{\partial t}+v_x\frac{\partial}{\partial x}+v_\theta\frac{\partial}{\partial\theta}+v_z\frac{\partial}{\partial z}, \quad (19)$$

At the point of contact between the fluid and the core, the relative velocity and acceleration in the radial direction are equal. So (Rabani Bidgoli *et al*. 2016)

$$v_z=\frac{dw}{dt}, \quad (20)$$

By employing Eqs. (19) and (20) and substituting into Eq. (18), the pressure inside the pipe can be computed as

$$\frac{\partial p_z}{\partial z}=-\rho_f\left(\frac{\partial^2 w}{\partial t^2}+2v_x\frac{\partial^2 w}{\partial x\,\partial t}+{v_x}^2\frac{\partial^2 w}{\partial x^2}\right)$$
$$+\mu\left(\frac{\partial^3 w}{\partial x^2\,\partial t}+\frac{\partial^3 w}{R^2\,\partial\theta^2\,\partial t}+v_x\left(\frac{\partial^3 w}{\partial x^3}+\frac{\partial^3 w}{R^2\,\partial\theta^2\,\partial x}\right)\right), \quad (21)$$

By multiplying two sides of Eq. (21) in the inside area of the pipe (A), the radial force in the pipe is calculated as below

$$F_{fluid}=A\frac{\partial p_z}{\partial z}=-\rho_f\left(\frac{\partial^2 w}{\partial t^2}+2v_x\frac{\partial^2 w}{\partial x\,\partial t}+{v_x}^2\frac{\partial^2 w}{\partial x^2}\right)$$
$$+\mu\left(\frac{\partial^3 w}{\partial x^2\,\partial t}+\frac{\partial^3 w}{R^2\,\partial\theta^2\,\partial t}+v_x\left(\frac{\partial^3 w}{\partial x^3}+\frac{\partial^3 w}{R^2\,\partial\theta^2\,\partial x}\right)\right), \quad (22)$$

Finally, the external work due to the pressure of the fluid may be obtained as follows

$$W_f=\int(F_{fluid})w\,dA=\int\Bigg(-\rho_f\left(\frac{\partial^2 w}{\partial t^2}+2v_x\frac{\partial^2 w}{\partial x\,\partial t}+{v_x}^2\frac{\partial^2 w}{\partial x^2}\right)$$
$$+\mu\left(\frac{\partial^3 w}{\partial x^2\,\partial t}+\frac{\partial^3 w}{R^2\,\partial\theta^2\,\partial t}+v_x\left(\frac{\partial^3 w}{\partial x^3}+\frac{\partial^3 w}{R^2\,\partial\theta^2\,\partial x}\right)\right)\Bigg)w\,dA, \quad (23)$$

Also, the external work due to outside fluid can be obtained as follows (Ghavanloo and Fazelzadeh 2011)

$$F_v=-\alpha\frac{\partial w}{\partial t}, \quad (24)$$

where

$$\alpha=\frac{2\nu_f\pi(\eta^2-1)}{(1-\eta^2+(\eta^2+1)\ln\eta)}\ \ and\ \eta=\frac{R_0}{R_1} \quad (25)$$

It should be noted that the parameter α is positive ($0<\eta<1$). Here, R_0 is shell outer radius and R_1 is the distance from the center line to the position where the induced viscous flow vanished. To couple the elastic deformation of the shell and the viscous flow of the external fluid, it is assumed that the surface traction of the external fluid along the interface is equal to external force exerted on the shell.

$$q=F_v \quad (26)$$

The external work due to the earthquake loads can be computed as below

$$W_s = \int (\underbrace{ma(t)}_{F_{Seismic}}) w dA, \tag{27}$$

Where m and $a(t)$ are the mass and the acceleration of the ground.

3.2 Hamilton's principle

The governing equations of the structure are derived using the Hamilton's principle which is considered as follows

$$\int_0^t (\delta U - \delta K - \delta W) dt = 0. \tag{28}$$

Now, by applying the Hamilton's principle and after integration by part and some algebraic manipulation, three equations of motion can be derived as follows

$$\frac{\partial N_x}{\partial x} + \frac{\partial N_{x\theta}}{R\partial\theta} = \rho h \frac{\partial^2 u}{\partial t^2}, \tag{29}$$

$$\frac{\partial N_\theta}{R\partial\theta} + \frac{\partial N_{x\theta}}{\partial x} = \rho h \frac{\partial^2 v}{\partial t^2}, \tag{30}$$

$$\begin{aligned} &\frac{\partial^2 M_x}{\partial x^2} + \frac{2\partial^2 M_{x\theta}}{R\,\partial x\,\partial\theta} + \frac{\partial^2 M_\theta}{R^2\,\partial\theta^2} - \frac{N_\theta}{R} + N_x \frac{\partial^2 w}{\partial x^2} + N_\theta \frac{\partial^2 w}{R^2 \partial\theta^2} \\ &+ N_{x\theta} \frac{2\partial^2 w}{R\partial x\,\partial\theta} + F_V + F_{fluid} = \rho h \frac{\partial^2 w}{\partial t^2} + F_{Seismic}, \end{aligned} \tag{31}$$

By integrating the stress-strain relations of the structure and introduced Eqs. (12)-(13), we have

$$\begin{aligned} N_x = h\Bigg(& C_{11}\left(\frac{\partial u}{\partial x} + 0.5\left(\frac{\partial w}{\partial x}\right)^2\right) \\ & + C_{12}\left(\frac{\partial v}{R\partial\theta} + \frac{w}{R} + 0.5\left(\frac{\partial w}{R\partial\theta}\right)^2\right)\Bigg), \end{aligned} \tag{32}$$

$$\begin{aligned} N_\theta = h\Bigg(& C_{12}\left(\frac{\partial u}{\partial x} + 0.5\left(\frac{\partial w}{\partial x}\right)^2\right) \\ & + C_{22}\left(\frac{\partial v}{R\partial\theta} + \frac{w}{R} + 0.5\left(\frac{\partial w}{R\partial\theta}\right)^2\right)\Bigg), \end{aligned} \tag{33}$$

$$N_{x\theta} = h\left(C_{66}\left(\frac{\partial u}{R\partial\theta} + \frac{\partial v}{\partial x} + \frac{\partial w}{R\partial\theta}\frac{\partial w}{\partial x}\right)\right), \tag{34}$$

$$M_x = \frac{h^3}{12}\left(C_{11}\left(-z\frac{\partial^2 w}{\partial x^2}\right) + C_{12}\left(-z\frac{\partial^2 w}{R^2\,\partial\theta^2}\right)\right), \tag{35}$$

$$M_\theta = \frac{h^3}{12}\left(C_{12}\left(-z\frac{\partial^2 w}{\partial x^2}_{\,x}\right) + C_{22}\left(-z\frac{\partial^2 w}{R^2\,\partial\theta^2}\right)\right), \tag{36}$$

$$M_{x\theta} = \frac{h^3}{12} C_{66}\left(-2z\frac{\partial^2 w}{R\,\partial\theta\,\partial x}\right). \tag{37}$$

By substituting stress resultants, Eqs. (32)-(37), in governing equations, Eqs. (29)-(31), relations can be obtained in terms of only the displacement fields.

Also, the boundary conditions are taken into account as below

Clamped-Clamped supported

$$\begin{aligned} & w = v = u = 0 \qquad @ \quad x = 0, L \\ & \frac{\partial w}{\partial x} = 0 \qquad @ \quad x = 0, L \end{aligned} \tag{38}$$

Simply-Simply supported

$$\begin{aligned} & w = v = \frac{\partial^2 w}{\partial x^2} = 0 \qquad @ \quad x = 0 \\ & w = v = \frac{\partial^2 w}{\partial x^2} = 0 \qquad @ \quad x = L \end{aligned} \tag{39}$$

Clamped-Simply supported

$$\begin{aligned} & w = v = u = \frac{\partial w}{\partial x} = 0 \qquad @ \quad x = 0 \\ & w = v = \frac{\partial^2 w}{\partial x^2} = 0 \qquad @ \quad x = L \end{aligned} \tag{40}$$

in the following, DQ method along with Newmark technique is selected because the governing equations are nonlinear and the higher accuracy is needed.

3.3 DQ method

There are a lot of numerical methods to solve the initial and/or boundary value problems that occur in an engineering domain. One of the best numerical methods is differential quadrature method (DQM).This method has several advantages compared to other numerical methods that are listed as below:

1. DQM is a precise method for solving of nonlinear differential equations in approximation of the derivatives.
2. DQM can satisfy a variety of boundary conditions and need much less formulation and programming effort.
3. The accuracy and convergence of the DQM is high.

Due to the above outstanding merits of the DQM, in recent years, the method has become increasingly popular in the numerical solution of problems in analysis of structural and dynamical problems. In these method, the derivative of the function may be defined as follows (Kolahchi *et al*. 2015)

$$\frac{d^n f_x(x_i,\theta_j)}{dx^n} = \sum_{k=1}^{N_x} A_{ik}^{(n)} f(x_k,\theta_j) \qquad n = 1,...,N_x - 1. \tag{41}$$

$$\frac{d^m f_y(x_i,\theta_j)}{d\theta^m} = \sum_{l=1}^{N_\theta} B_{jl}^{(m)} f(x_i,\theta_l) \qquad m = 1,...,N_\theta - 1. \tag{42}$$

$$\frac{d^{n+m} f_{xy}(x_i,\theta_j)}{dx^n d\theta^m} = \sum_{k=1}^{N_x}\sum_{l=1}^{N_\theta} A_{ik}^{(n)} B_{jl}^{(m)} f(x_k,\theta_l). \tag{43}$$

where N_x and N_θ denote the number of points in x and θ directions, $f(x, \theta)$ is the function, and A_{ik}, B_{jl} are the weighting coefficients defined as

$$A_{ij}^{(1)}=\begin{cases}\dfrac{M(x_i)}{(x_i-x_j)M(x_j)} & for \quad i\neq j, \quad i,j=1,2,...,N_x\\ -\sum\limits_{\substack{j=1\\ i\neq j}}^{N_x}A_{ij}^{(1)} & for \quad i=j, \quad i,j=1,2,...,N_x\end{cases} \tag{44}$$

$$B_{ij}^{(1)}=\begin{cases}\dfrac{P(\theta_i)}{(\theta_i-\theta_j)P(\theta_j)} & for \quad i\neq j, \quad i,j=1,2,...,N_\theta,\\ -\sum\limits_{\substack{j=1\\ i\neq j}}^{N_\theta}B_{ij}^{(1)} & for \quad i=j, \quad i,j=1,2,...,N_\theta\end{cases} \tag{45}$$

where M and P are Lagrangian operators defined as

$$M(x_i)=\prod_{\substack{j=1\\ j\neq i}}^{N_x}(x_i-x_j) \tag{46}$$

$$P(\theta_i)=\prod_{\substack{j=1\\ j\neq i}}^{N_\theta}(\theta_i-\theta_j) \tag{47}$$

and for higher-order derivatives, we have

$$A_{ij}^{(n)}=n\left(A_{ii}^{(n-1)}A_{ij}^{(1)}-\frac{A_{ij}^{(n-1)}}{(x_i-x_j)}\right) \tag{48}$$

$$B_{ij}^{(m)}=m\left(B_{ii}^{(m-1)}B_{ij}^{(1)}-\frac{B_{ij}^{(m-1)}}{(\theta_i-\theta_j)}\right) \tag{49}$$

The Chebyshev polynomials are used as below for selecting sampling grid points

$$X_i=\frac{L}{2}\left[1-\cos\left(\frac{i-1}{N_x-1}\right)\pi\right] \qquad i=1,...,N_x \tag{50}$$

$$\theta_i=\frac{2\pi}{2}\left[1-\cos\left(\frac{i-1}{N_\theta-1}\right)\pi\right] \qquad i=1,...,N_\theta \tag{51}$$

Assuming Eqs. (52)-(54) (for changing relations to standard eigenvalue problem form) and applying above equations into the motion equations, the matrix form of governing equations can be written as Eq. (53)

$$\bar{u}(x,y,t)=\bar{u}(x,y)e^{\lambda\bar{t}}, \tag{52}$$

$$\bar{v}(x,y,t)=\bar{v}(x,y)e^{\lambda\bar{t}}, \tag{53}$$

$$\bar{w}(x,y,t)=\bar{w}(x,y)e^{\lambda\bar{t}}, \tag{54}$$

$$\left(\left[\underbrace{K_L+K_{NL}}_{K}\right]+\Omega[C]+\Omega^2[M]\right)\begin{Bmatrix}\{d_b\}\\ \{d_d\}\end{Bmatrix}=\begin{Bmatrix}\{0\}\\ -Ma(t)\end{Bmatrix}, \tag{55}$$

where K_L, K_{NL}, C, M, d_b and d_d represent the linear stiffness matrix, the nonlinear stiffness matrix, the damping matrix, the mass matrix, the boundary points and domain points, respectively.

3.4 Newmark method

Newmark-β method can be employed to obtain the time response of the structure. Based on this method, Eq. (55) can be rewritten as below (Simsek 2010)

$$K^*(d_{i+1})=Q_{i+1}, \tag{56}$$

$K^*(di+1)$ and Q_{i+1} are the effective stiffness matrix and the effective load vector in time of $i+1$ which can be presented as

$$K^*(d_{i+1})=K_L+K_{NL}(d_{i+1})+\alpha_0M+\alpha_1C, \tag{57}$$

$$Q_{i+1}^*=Q_{i+1}+M\left(\alpha_0d_i+\alpha_2\dot{d}_i+\alpha_3\ddot{d}_i\right)+C\left(\alpha_1d_i+\alpha_4\dot{d}_i+\alpha_5\ddot{d}_i\right), \tag{58}$$

and

$$\begin{gathered}\alpha_0=\frac{1}{\chi\Delta t^2}, \qquad \alpha_1=\frac{\gamma}{\chi\Delta t}, \qquad \alpha_2=\frac{1}{\chi\Delta t},\\ \alpha_3=\frac{1}{2\chi}-1, \quad \alpha_4=\frac{\gamma}{\chi}-1,\\ \alpha_5=\frac{\Delta t}{2}\left(\frac{\gamma}{\chi}-2\right), \ \alpha_6=\Delta t(1-\gamma), \quad \alpha_7=\Delta t\gamma,\\ \gamma=0.5, \qquad \chi=0.25\end{gathered} \tag{59}$$

Eq. (56) is solved at any time step and modified velocity and acceleration vectors are calculated as follows

$$\ddot{d}_{i+1}=\alpha_0(d_{i+1}-d_i)-\alpha_2\dot{d}_i-\alpha_3\ddot{d}_i, \tag{60}$$

$$\dot{d}_{i+1}=\dot{d}_i+\alpha_6\ddot{d}_i+\alpha_7\ddot{d}_{i+1}, \tag{61}$$

these modified velocity and acceleration in Eqs. (60) and (61) are considered in next time step and all these procedures mentioned above are repeated.

4. Numerical results and discussion

A computer program based on the DQM being written in MATLAB to solve the nonlinear motion equations set out originally in Eq. (56). For this purpose, a nanocomposite pipe of length a, radius Rand thickness h as shown in Fig. 1 is considered. Also, it is assumed the flowing liquid is water. The mass density and viscosity of water is equal to (9982 Kg/m^3) and (10^{-3} Pas) respectively. Also, for the strengthening of concrete, SiO_2 nanoparticles with the density of ρ_{np}=3970 Kg/m^3 is used. For considering earthquake effects, the acceleration of the earthquake according to Tabas earthquake is considered that the distribution of acceleration in 20 seconds is shown in Fig. 2. Furthermore, the cylindrical shell is investigated with three kinds of boundary conditions: two edges simply supported (SS), clamped (CC), and simply supported and clamped (SC).

4.1 Validation

In the absence of similar publications in the literature covering the same scope of the problem, one can not directly validate the results found here. Therefore, the present work could be partially validated based on a simplified analysis without considering the nonlinear terms

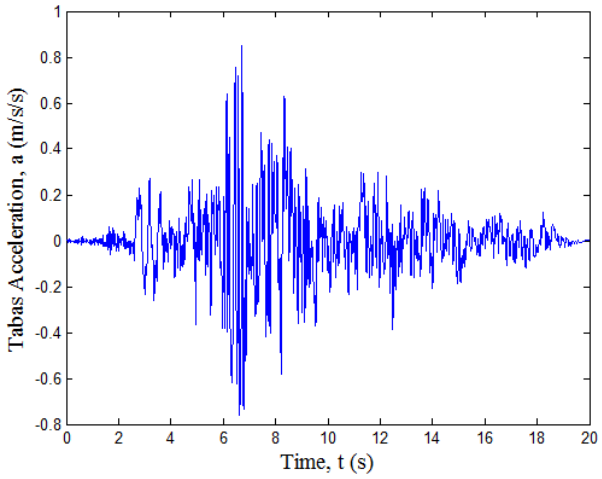

Fig. 2 The accelerogram of 1978 Tabas Earthquake

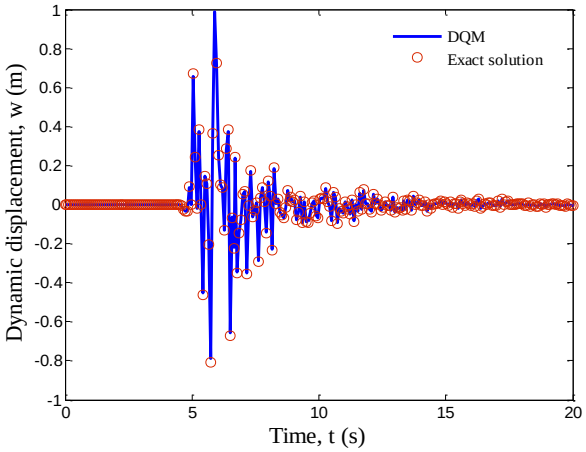

Fig. 3 Comparison of the present work with the Exact solution

of the governing equations and by comparing the linear dynamic response of the pipe which obtained by two various solution methods. It can be concluded that DQM method is accurate and acceptable for present problem because the present results closely match with the analytical method illustrated in Fig. 3.

4.2 The convergence of present method

The convergence and accuracy of DQ method in evaluating the maximum deflection of the underwater pipe conveying fluid is illustrated in Fig. 4. The results are offered for different values of the DQM grid points. It is found that 15 DQ grid points can yield accurate results. So, the results presented below are based on the number of grid points 15 for DQ solution method.

4.3 Effect of various parameters

In this study, four types of pipelines considering the existence of external and internal fluid were modeled and computed. Fig. 5 shows the dynamic displacement of submerged pipeline under Tabas earthquake for two cases of empty and fluid-conveying pipeline with dashed and solid

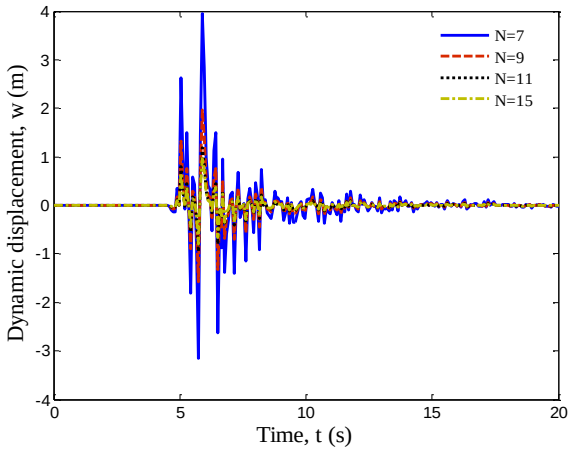

Fig. 4 Accuracy of DQM for determining the dynamic displacement

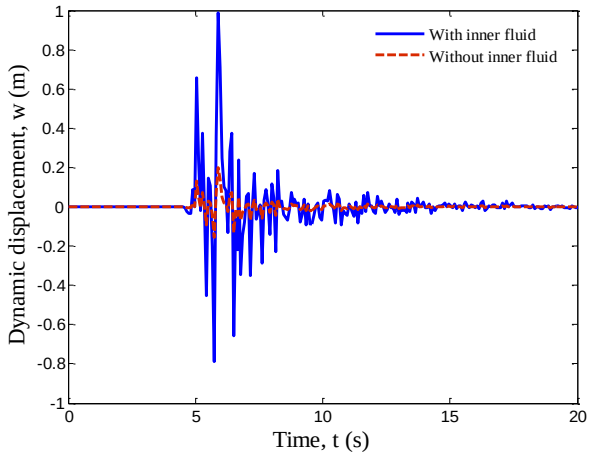

Fig. 5 The effect of internal fluid on the dynamic displacement of submerged pipe versus time

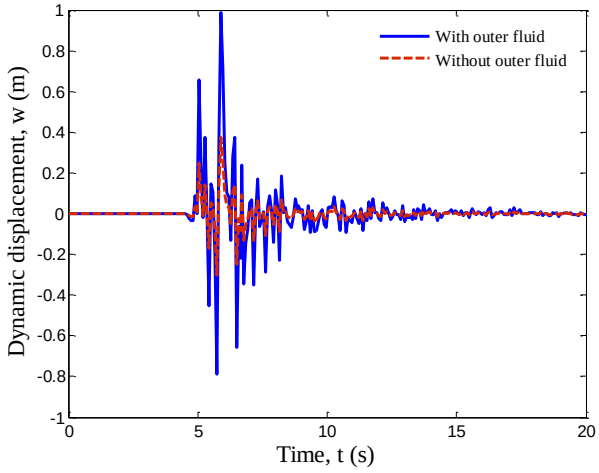

Fig. 6 The effect of external fluid on the dynamic displacement of fluid-conveying pipe versus time

lines, respectively. It can be found that considering the interior fluid, decreases the stiffness of the structure and as a result, the displacement of the structure increases. Furthermore, the maximum displacement value for the submerged pipeline conveying fluid is almost five times

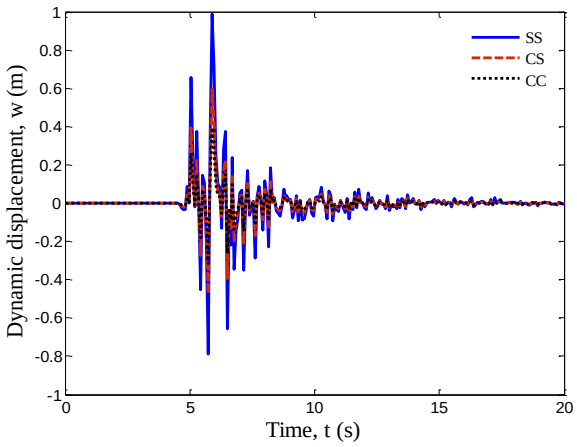

Fig. 7 The boundary conditions effects on the dynamic displacement versus time

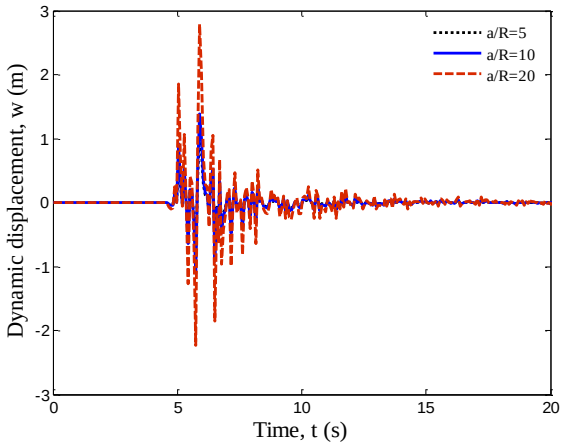

Fig. 9 The effect of length to radius ratio of pipe on the dynamic response of pipe versus time

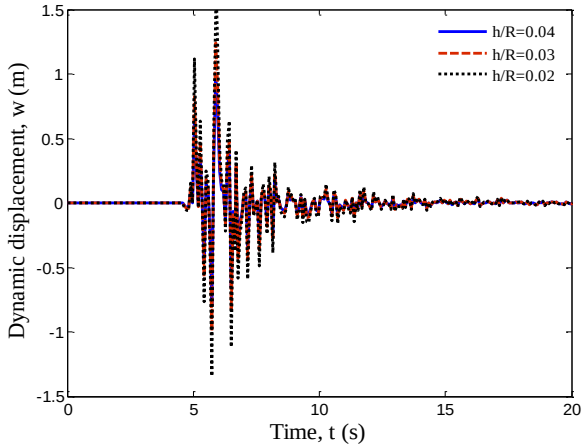

Fig. 8 The effect of thickness to radius ratio on the dynamic response of pipe versus time

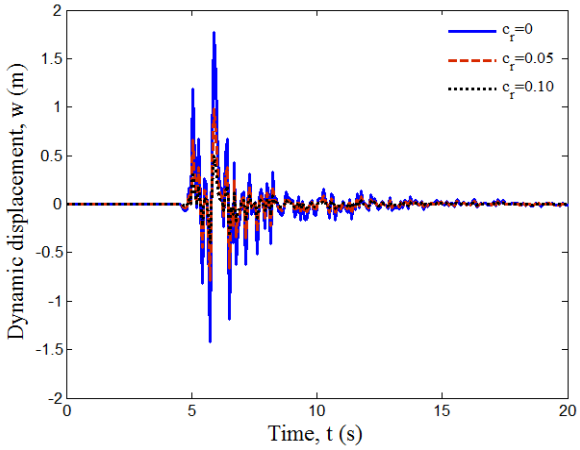

Fig. 10 The effect of SiO_2 nano-particles volume percent on the dynamic response of pipe versus time

more than the submerged pipeline without fluid.

The dynamic displacement of pipeline conveying fluid under Tabas earthquake for two cases of the existence of external fluid and without external fluid is shown in Fig. 6. It can be observed in the presence of external fluid, dynamic deflection of system increases because the stiffness of the structure decreases. Also, the maximum deflection value for the submerged pipeline conveying fluid is almost three times more than the pipeline conveying fluid without external fluid. By comparing Figs. 5 and 6, it can be observed that the maximum deflection for the submerged pipeline without internal fluid is less than the pipeline conveying fluid without external fluid.

The changes of deflection versus time for various boundary conditions are shown in Fig. 7. By investigating the boundary conditions effects on the dynamic displacement of the structure, it is found that the pipe with simply-simply boundary condition has the most deflection in comparison to the other ones. Because the simply boundary condition has lower constraint and consequently the structure is softer.

Fig. 8 indicates the effect of the thickness to radius ratio on the dynamic deflection versus time. As can be seen, by increasing the thickness of the structure, dynamic deflection of system decreases. it is because the structure become stiffer.

The effect of aspect ratio (a/R) on the dynamic deflection versus time is shown in Fig. 9. It is obvious that by increasing the length to radius ratio, the dynamic deflection of system increases.

The effect of SiO_2 nanoparticles volume percent on the dynamic displacement of the system versus time is shown in Fig. 10. The changes of the displacement are shown for C_r=0, C_r=0.05 and C_r=0.10. The results show that increasing of SiO_2 nanoparticles volume percent leads to decreasing in dynamic deflection of the system for the reason that the stiffness of the structure increases.

5. Conclusions

The dynamic response of nanocomposite submerged pipeline conveying fluid under the earthquake acceleration was investigated in this study. The nanotechnology was used for improving the mechanical behavior of Concrete pipe and it was strengthened with SiO_2 nanoparticles. The Mori-Tanaka method was applied for determining the elastic coefficients of nanocomposite. Furthermore, the

system was subjected to the dynamic loads caused by earthquake. Navier-Stokes equation and an external force were employed to calculate the internal and external fluid effect in the pipe, respectively. The motion equations were derived using an energy method and Hamilton's principle and solved via DQM and Newmark method. The effects of boundary conditions, volume percent of SiO_2 nanoparticles, geometrical parameters of pipe and the interior and exterior fluid force on the dynamic displacement of the structure for the Tabas earthquake were taken into considerations. Results indicate:

1-The present results obtained by DQM and Newmark method are in good agreement with analytical method.

2-With Increasing the SiO_2 nanoparticles volume percent, the dynamic deflection of the system decreases because the stiffness of the structure increases.

3-Considering the interior fluid in the submerged pipeline, decreases the stiffness of the structure and as a result, the displacement of the structure almost five times increases.

4-External fluid force in the pipeline conveying fluid, causes the dynamic deflection of system almost three times increases because the stiffness of the structure decreases.

5-The maximum deflection for the submerged pipeline without internal fluid is less than the pipeline conveying fluid without external fluid.

6-The lowest and highest dynamic deflection of the structure were respectively obtained for simply-simply and clamped-clamped boundary condition.

7-By increasing the length to radius ratio of pipe, the dynamic deflection of system increases. It is because the structure become softer.

8-By increasing the thickness to radius ratio, dynamic deflection of system decreases. It is because the structure become stiffer.

References

Abdoun, T.H., Ha, D., O'Rourke, M., Symans, M., O'Rourke, T., Palmer, M. and Harry, E. (2009), "Factors influencing the behavior of buried pipelines subjected to earthquake faulting", *Soil Dyn. Earthq. Eng.*, **29**, 415-427.

Alijani, F. and Amabili, M. (2014), "Nonlinear vibrations and multiple resonances of fluid filled arbitrary laminated circular cylindrical shells", *Compos. Struct.*, **108**, 951-962.

Amabili, M. (2008), *Nonlinear Vibrations and Stability of Shells and Plates*, Cambridge University Press, Cambridge.

Amabili, M. and Païdoussis, M.P. (2003), "Review of studies on geometrically nonlinear vibrations and dynamics of circular cylindrical shells and panels, with and without fluid-structure interaction", *Appl. Mech. Rev.*, **56**, 349-381.

Amabili, M., Pellicano, F. and Païdoussis, M.P. (1999a), "Non-linear dynamics and stability of circular cylindrical shells containing flowing fluid Part I: stability", *J. Sound Vib.*, **225**, 655-699.

Amabili, M., Pellicano, F. and Païdoussis, M.P. (1999b), "Non-linear dynamics and stability of circular cylindrical shells containing flowing fluid Part II: large-amplitude vibrations without flow", *J. Sound Vib.*, **228**, 1103-1124.

Amabili, M., Pellicano, F. and Païdoussis, M.P. (2000), "Non-linear dynamics and stability of circular cylindrical shells containing flowing fluid. Part III: truncation effect without flow and experiments", *J. Sound Vib.*, **237**, 617-640.

Benjamin, T.B. (1961), "Dynamics of a system of articulated pipes conveying fluid", *Proc. Royal Soc. A.*, **261**(130), 457-486.

Brush, O. and Almorth, B. (1975), *Buckling of Bars, Plates and Shells*, Mc-Graw Hill.

Chen, W., Shih, B.J., Chen, Y.C., Hung, J.H. and Hwang, H.H. (2002), "Seismic response of natural gas and water pipelines in the Ji-Ji earthquake", *Soil Dyn. Earthq. Eng.*, **22**, 1209-1214.

Dey, T. and Ramachandra, L.S. (2017), "Non-linear vibration analysis of laminated composite circular cylindrical shells", *Compos. Struct.*, **163**, 89-100.

Ghavanloo, E. and Fazelzadeh, A. (2011), "Flow-thermoelastic vibration and instability analysis of viscoelastic carbon nanotubes embedded in viscous fluid", *Physica E.*, **44**, 17-24.

GhorbanpourArani, A., Bagheri, M.R., Kolahchi, R. and KhodamiMaraghi, Z. (2013), "Nonlinear vibration and instability of fluid-conveying DWBNNT embedded in a visco-Pasternak medium using modified couple stress theory", *J. Mech. Sci. Tech.*, **27**(9), 2645-2658.

Gong, S.W., Lam, K.Y. and Lu, C. (2000), "Structural analysis of a submarine pipeline subjected to underwater shock", *Int. J. Pres. Ves. Pip.*, **77**, 417-423.

Housner, G.W. (1952), "Bending vibrations of a pipe line containing flowing fluid", *J. Appl. Mech.*, **19**, 205-208.

Huang, Y.M., Liu, Y.S., Li, B.H., Li, Y.J. and Yue, Z.F. (2010), "Natural frequency analysis of fluid conveying pipeline with different boundary conditions", *Nucl. Eng. Des.*, **240**(3), 461-467.

Inozemtcev, A.S., Korolev, E.V. and Smirnov, V.A. (2017), "Nanoscale modifier as an adhesive for hollow microspheres to increase the strength of high-strength lightweight concrete", *Struct. Concrete*, **18**(1), 67-74.

JafarianArani, A and Kolahchi, R. (2016), "Buckling analysis of embedded concrete columns armed with carbon nanotubes", *Comput. Concrete*, **17**(5), 567-578.

Kolahchi, R., RabaniBidgoli, M., Beygipoor, G.H. and Fakhar, M.H. (2015), "A nonlocal nonlinear analysis for buckling in embedded FG-SWCNT-reinforced microplates subjected to magnetic field", *J. Mech. Sci. Tech.*, **29**, 3669-3677.

Lam, K.Y., Zong, Z. and Wang, Q.X. (2003), "Dynamic response of a laminated pipeline on the seabed subjected to underwater shock", *Compos. Part B-Eng.*, **34**, 59-66.

Lee, U. and Oh, H. (2003), "The spectral element model for pipelines conveying internal steady flow", *Eng. Struct.*, **25**, 1045-1055.

Li, Ch., Zhang, Y., Tu, W., Jun, C., Liang, H. and Yu, H. (2017), "Soft measurement of wood defects based on LDA feature fusion and compressed sensor images", *J. Forest. Res.*, **28**, 1285-1292.

Lin, W. and Qiao, N. (2008), "Vibration and stability of an axially moving beam immersed in fluid", *Int. J. Solid. Struct.*, **45**, 1445-1457.

Liu, H., Ma, J. and Huang, W. (2018), "Sensor-based complete coverage path planning in dynamic environment for cleaning robot", *CAAI Trans. Intell. Technol.*, **3**, 65-72.

Liu, Z.G., Liu, Y. and Lu, J. (2012), "Fluid-structure interaction of single flexible cylinder in axial flow", *Comput. Fluid.*, **56**, 143-151.

Lopes, J.L., Païdoussis, M.P. and Semler, C. (2002), "Linear and nonlinear dynamics of cantilevered cylinders in axial flow part 2: the equations of motion", *J. Fluid Struct.*, **16**, 715-737.

Mori, T. and Tanaka, K. (1973), "Average stress in matrix and average elastic energy of materials with misfitting inclusions", *Acta. Metall. Mater.*, **21**, 571-574.

Motezaker, M. and Kolahchi, R. (2017), "Seismic response of SiO_2 nanoparticles-reinforced concrete pipes based on DQ and

newmark methods", *Comput. Concrete*, **19**(6), 745-753.
Padhy, S. and Panda, S. (2017), "A hybrid stochastic fractal search and pattern search technique based cascade PI-PD controller for automatic generation control of multi-source power systems in presence of plug in electric vehicles", *CAAI Trans. Intell. Technol*., **2**, 12-25.
Païdoussis, M.P. (2004), *Fluid-Structure Interactions, Slender Structures and Axial Flow*, Vol. 2, Elsevier Academic Press, London.
Païdoussis, M.P. (2005), "Some unresolved issues in fluid-structure interactions", *J. Fluid Struct.*, **20**, 871-890.
Paidoussis, M.P. and Issid, N.T. (1974), "Dynamic stability of pipes conveying fluid", *J. Sound Vib.*, **33**, 267-294.
Païdoussis, M.P., Grinevich, E., Adamovic, D. and Semler, C. (2007a), "Linear and nonlinear dynamics of cantilevered cylinders in axial flow part 1: physical dynamics", *J. Fluid Struct.*, **16**, 691-713.
Païdoussis, M.P., Semler, C., Wadham-Gagnon, M. and Saaid, S. (2007b), "Dynamics of cantilevered pipes conveying fluid part 2: dynamics of the system with intermediate spring support", *J. Fluid Struct.*, **23**, 569-587.
Rabani Bidgoli, M. and Saeidifar, M. (2017), "Time-dependent buckling analysis of SiO_2 nanoparticles reinforced concrete columns exposed to fire", *Comput. Concrete*, **20**(2), 119-127.
Rabani Bidgoli, M., Karimi, M.S. and Ghorbanpour Arani, A. (2016), "Nonlinear vibration and instability analysis of functionally graded CNT-reinforced cylindrical shells conveying viscous fluid resting on orthotropic Pasternak medium", *Mech. Adv. Mater. Struct*., **23**(7), 819-831.
Ray, M.C. and Reddy, J.N. (2013), "Active damping of laminated cylindrical shells conveying fluid using 1-3 piezoelectric composites", *Compos. Struct.*, **98**, 261-271.
Rishikeshan, C.A. and Ramesh, H. (2017), "A novel mathematical morphology based algorithm for shoreline extraction from satellite images", *Geo-spatial Inform. Sci*., **20**, 345-352.
Safari Bilouei, B., Kolahchi, R. and Rabanibidgoli, M. (2016), "Buckling of concrete columns retrofitted with Nano-Fiber Reinforced Polymer (NFRP)", *Comput. Concrete*, **18**(5), 1053-1063.
Semler, C., Lopes, J.L., Augu, N. and Païdoussis, M.P. (2002), "Linear and nonlinear dynamics of cantilevered cylinders in axial flow part 3: nonlinear dynamics", *J. Fluid Struct*., **16**, 739-759.
Shamsuddoha, M., Islam, M.M., Aravinthan, T., Manalo, A. and Lau, K.T. (2013), "Effectiveness of using fibre-reinforced polymer composites for underwater steel pipeline repairs", *Compos. Struct*., **100**, 40-54.
Shokravi M. (2017), "Vibration analysis of silica nanoparticles-reinforced concrete beams considering agglomeration effects", *Comput. Concrete*, **19**(3), 333-338.
Simsek, M. (2010), "Non-linear vibration analysis of a functionally graded Timoshenko beam under action of a moving harmonic load", *Compos. Struct*., **92**, 2532-2546.
Su, Y., Li, J., Wu, C and Li, Z.X. (2016), "Influences of nano-particles on dynamic strength of ultra-high performance concrete", *Compos. Part B-Eng*., **91**, 595-609.
Thinh, T.I. and Nguyen, M.C. (2016), "Dynamic stiffness method for free vibration of composite cylindrical shells containing fluid", *Appl. Math. Model*., **40**, 9286-9301.
Torres-Jimenez, J. and Rodriguez-Cristerna, A. (2017), "Metaheuristic post-optimization of the NIST repository of covering arrays", *CAAI Trans. Intell. Technol*., **2**, 31-38.
Wadham-Gagnon, M., Païdoussis, M.P. and Semler, C. (2007), "Dynamics of cantilevered pipes conveying fluid part 1: nonlinear equations of three-dimentional motion", *J. Fluid Struct.*, **23**, 545-67.
Wen, Q., He, J., Guan, Sh., Chen, T., Hu, Y., Wu, W., Liu, F., Qiao, Y. (2017), "The TripleSat constellation: a new geospatial data service model", *Geo-spatial Inform. Sci.*, **20**, 163-173.
Yang, H. and Yu, L. (2017), "Feature extraction of wood-hole defects using wavelet-based ultrasonic testing", *J. Forest. Res*., **28**, 395-402.
Yoon, H.I. and Son, I. (2007), "Dynamic response of rotating flexible cantilever fluid with tip mass", *Int. J. Mech. Sci*., **49**, 878-887.
ZamaniNouri, A. (2017), "Mathematical modeling of concrete pipes reinforced with CNTs conveying fluid for vibration and stability analyses", *Comput. Concrete*, **19**(3), 325-331.
Zhai, H., Wu, Z., Liu, Y. and Yue, Z. (2011), "Dynamic response of pipeline conveying fluid to random excitation", *Nucl. Eng. Des.*, **241**, 2744-2749.
Zhao, B., Gao, L., Liao, W. and Zhang, B. (2017), "A new kernel method for hyperspectral image feature extraction", *Geo-spatial Inform. Sci.*, **20**, 309-318.
Zhou, X.Q., YU, D.Y., Shao, X.Y., Zhang, C.Y. and Wang, S. (2017), "Dynamics characteristic of steady fluid conveying in the periodical partially viscoelastic composite pipeline", *Compos. Part B-Eng*., **111**, 387-408.

CC